NASA Contractor Report 3636

Wind-Tunnel Investigation of Effects of Wing-Leading-Edge Modifications on the High Angle-of-Attack Characteristics of a T-Tail Low-Wing General-Aviation Aircraft

E. Richard White

CONTRACT NAS1-16000
NOVEMBER 1982

NASA

NASA Contractor Report 3636

Wind-Tunnel Investigation of Effects of Wing-Leading-Edge Modifications on the High Angle-of-Attack Characteristics of a T-Tail Low-Wing General-Aviation Aircraft

E. Richard White
Kentron International, Inc.
Hampton, Virginia

Prepared for
Langley Research Center
under Contract NAS1-16000

National Aeronautics
and Space Administration

**Scientific and Technical
Information Branch**

1982

SUMMARY

Exploratory tests have been conducted in the NASA-Langley Research Center's 12-Foot Low-Speed Wind Tunnel to evaluate the application of wing-leading-edge devices on the stall-departure and spin resistance characteristics of a 1/6-scale model of a T-tail general-aviation aircraft. The model was force tested with an internal strain-gauge balance to obtain aerodynamic data on the complete configuration and with a separate wing balance to obtain aerodynamic data on the outer portion of the wing.

The addition of the outboard leading-edge droop eliminated the abrupt stall of the wingtip and maintained or increased the resultant-force coefficient up to about α = 32 degrees. This change in slope of the resultant-force coefficient curve with angle of attack from negative to positive values at higher angles of attack has been shown to be important for eliminating autorotation and for providing spin resistance.

INTRODUCTION

The NASA/Langley Research Center is currently engaged in a research effort to develop the technology required to improve the stall/spin characteristics of light general-aviation aircraft. This effort has involved various test techniques such as small-scale and full-scale wind-tunnel tests, radio-controlled model flight tests, and full-scale flight tests. Several different aircraft configurations have been evaluated and the results are documented in references 1 through 9.

These results have shown that one concept which proved extremely effective for improving the stall characteristics and spin resistance of low-wing general-aviation aircraft consists of an outboard-droop modification to the wing leading edge. Previous work has been limited to untapered wing configurations such as described in references 1 through 6. The objective of the present investigation was to determine the effectiveness of the outboard leading-edge droop modification on a low-wing T-tail configuration with a tapered outer-wing panel.

A summary of the significant results obtained on the effects of wing leading-edge modifications on the stall/spin behavior of a low-wing general-aviation research airplane is given in reference 5. Of particular interest to the present investigation is the classical interpretation of static aerodynamic data to estimate stable and unstable boundaries for the damping-in-roll characteristics of straight wings near the stall. The relationship between autorotative tendencies and variations of C_L and C_D with angle of attack was defined in early research by Glauert (reference 10) and Knight (reference 11). As discussed in reference 11, strip theory analysis indicates that autorotation is encountered when the variation of the total resultant-force coefficient of a wing with angle of attack (the slope of the resultant-force curve) becomes negative. More recent studies, such as those of reference 6, have shown that improved definition of autorotative tendencies can be obtained by considering the aerodynamics of the outer-wing panel and its resultant-force coefficient variation with angle of attack. Therefore, the current tests employ a three-component balance mounted at the wing semispan to measure the outer-wing panel aerodynamic forces. A standard six-component strain-gauge balance was used to measure the aerodynamic forces and moments of the complete configuration. Tests were conducted for the basic unmodified configuration, and for the configuration with various lengths of outboard leading-edge droop, a full-span droop, and a faired droop. Both longitudinal and lateral-directional data were obtained as well as aileron control effectiveness information. Full-scale flight tests of the aircraft were conducted in a separate investigation to evaluate the basic and outboard leading-edge droop aircraft configurations developed during the force-test program.

SYMBOLS

The longitudinal aerodynamic coefficients are referred to the stability-axes system while lateral-directional aerodynamic coefficients are referred to the body-axes system. The moment center was located at 27-percent of the mean aerodynamic chord, which is the defined aft CG limit of the aircraft. Dimensional quantities are presented in U.S. Customary Units.

b wing span (ft)

C_D drag coefficient, $\frac{\text{drag}}{qS}$

C_L lift coefficient, $\frac{\text{lift}}{qS}$

C_ℓ rolling-moment coefficient, $\frac{\text{rolling moment}}{qSb}$

C_{ℓ_β} rolling-moment coefficient due to sideslip, per deg

C_m pitching moment coefficient, $\frac{\text{pitching moment}}{qSc}$

C_n yawing-moment coefficient, $\frac{\text{yawing moment}}{qSb}$

C_{n_β} yawing-moment coefficient due to sideslip, per deg

C_R resultant-force coefficient, $\sqrt{C_L^2 + C_D^2}$

C_{R_α} slope of resultant-force curve, $\frac{\partial C_R}{\partial \alpha}$, per deg

$\bar{c}$ mean aerodynamic chord, ft

i local incidence (twist), deg

q freestream dynamic pressure, lb/ft^2

S wing reference area, ft^2

α angle of attack, deg

β angle of sideslip, deg

δ_a aileron deflection angle, deg

δ_e elevator deflection angle, deg

Abbreviations:

WB outer-wing panel balance data

CG center of gravity

MODEL DESCRIPTION AND TESTS

The 1/6-scale model used in the tests was a fiberglass and wood replica of a low-wing T-tail general-aviation research aircraft. Figure 1 shows a sketch of the configuration and its dimensional characteristics. Figure 2 shows a sketch of the leading-edge droop cross section, and the coordinates of the section are listed in table 1. This droop geometry is similar to that used in the studies discussed in reference 5. A photo of the model installed in the 12-foot low-speed wind tunnel is shown in figure 3. The wing outboard-droop developed in this investigation may also be seen on the model in figure 3.

The tests were conducted in the Langley 12-Foot Low-Speed Wind Tunnel which has an octagonal test section. The free-stream dynamic pressure of the test was 4 lb/ft^2 which corresponds to a Reynolds number of 320,000 based on the wing mean aerodynamic chord of 0.864 feet. Data were obtained over an angle-of-attack range of -4 to 60 degrees for sideslip angles of -8 to +8 degrees.

The model was mounted on a six-component strain-gauge balance for measuring total configuration forces and moments. A three-component balance was mounted at the wing semi-span station to measure outer panel lift, drag, and rolling moment. No corrections were made or needed due to jet boundary effects or blockage since the model was small relative to tunnel size.

Configurations tested included: (1) the basic model, (2) the model with a full-span leading-edge droop, (3) the model with several different spanwise lengths of outboard leading-edge droop, and (4) the model with an outboard droop

faired smoothly into the wing leading edge to eliminate the discontinuity of the leading edge. Several leading-edge droops of different cross-sections were evaluated during the investigation; however, the data presented here are limited to the leading-edge droop geometry which demonstrated the most favorable aerodynamic characteristics and minimum drag penalty.

RESULTS AND DISCUSSION

Longitudinal Characteristics

Presented in figure 4 is the variation of total lift and outer panel resultant-force coefficient as a function of angle of attack for the configuration with the basic wing, with outboard leading-edge droop, with full-span leading-edge droop, and with a faired outboard leading-edge droop. The data of figure 4 show that the aerodynamic characteristics of the configuration at high angles of attack were generally determined by the outer-wing panels. The inboard-wing stall can be observed at an angle of attack of about 12 degrees for all configurations except for the full-span leading-edge droop which stalled at about 14 degrees. The wing-tip stall for the basic wing occurred at an angle of attack of 18 degrees in both the lift and resultant-force data. The addition of the outboard leading-edge droop is shown to eliminate the abrupt stall of the wingtip and to maintain or increase the resultant-force coefficient up to about α = 32 degrees. This change in slope of the resultant-force coefficient curve with angle of attack from negative to positive values at higher angles of attack has been shown to be important for eliminating autorotation and for providing spin resistance. It is interesting to note that the addition of a fairing to the outboard droop (to eliminate the leading-edge discontinuity), or the addition of a full-span leading-edge droop, lowered the angle of attack at which the

outer panel stalled, and thus, degraded the effectiveness of the outboard-droop modification.

In order to determine the optimum length of the outboard leading-edge droop, a series of different lengths of droop was tested. From these data the critical angle of attack was established as the maximum angle of attack at which a positive slope of the resultant-force curve was obtained. Presented in figure 5 is a plot of critical angle of attack as a function of the leading-edge droop discontinuity location. It can be seen that the location of the outboard-droop discontinuity at a span station, $y/b/2$, of 0.55 to 0.60 provided the most favorable outer-panel aerodynamics. The outboard-droop geometry starting at $y/b/2 = 0.55$ is considered the baseline outboard-droop discussed in this investigation.

Shown in figure 6 are tuft photographs of the basic wing and outboard-droop configurations for an angle-of-attack range from 0° to 32°. The progression of the stall from the wing root toward the tip may be seen for both configurations. At about 20° angle of attack, the outward increase in flow separation on the outer panel is very evident on the basic configuration, while attached flow is maintained to some degree on the wing tips through 28° for the outboard-droop configuration. These tuft photographs illustrate the effectiveness of the outboard-droop in maintaining attached flow on the wingtips and provide flow characteristics for interpreting the aerodynamic data of figures 4 and 5.

A primary consideration in predicting whether the outboard-droop modification will provide stall departure resistance in flight depends to a large degree on whether the aircraft has enough elevator power to trim the configuration in pitch to angles of attack beyond the stall of the outer panel. Figure 7 shows

pitching-moment data for the basic and outboard leading-edge droop configurations for neutral elevator and full-up elevator inputs. The data of figure 7 are referred to the most aft center of gravity designated for the full-scale aircraft. It may be seen that while the basic configuration can be trimmed beyond the stall angle of the outer panel, the elevator cannot trim the outboard-droop configuration up to the stall angle of attack. This result would indicate that at this center-of-gravity location, the outboard-droop configuration should not depart at full-up elevator input. It should be noted, however, that the spin resistance of the configuration will depend upon the effectiveness of the elevator as well as other factors such as power effects and the aerodynamic moments due to rotational inputs such as during spin entries in determining the stall angle-of-attack margin on the outer portion of the wing.

Lateral-Directional Characteristics

Presented in figure 8 are lateral-directional stability data for the basic configuration and for the configuration with the outboard wing leading-edge droop modification. The data show the basic configuration has stable lateral-directional stability characteristics over the test angle-of-attack range. The addition of the outboard leading-edge droop adversely affected the directional stability parameter, C_{n_β}, at the higher angles of attack. The leading-edge droop, as expected, extended the angle of attack at which the effective dihedral parameter, C_{ℓ_β}, decreased, indicating an extension in angle of attack for wing stall. The data show that the leading-edge droop caused lateral instability after the wing stalled ($\alpha = 36°$).

Since the outboard leading-edge droop modification is effective in maintaining attached flow on the outer wing panel at higher angles of attack,

improved aileron effectiveness would be expected in the high angle-of-attack region. As can be seen in figure 9, additional rolling moments result from aileron deflection on the modified configuration in the angle-of-attack range prior to wing stall.

SUMMARY OF RESULTS

The results of tests to evaluate the application of wing leading-edge devices on the stall-departure and spin resistance characteristics of a 1/6-scale model of a T-tail general-aviation airplane showed that the addition of the outboard leading-edge droop eliminated the abrupt stall of the wingtip and maintained or increased the resultant-force coefficient up to about α = 32 degrees. This change in slope of the resultant-force coefficient curve with angle of attack from negative to positive values at higher angles of attack has been shown to be important for eliminating autorotation and for providing spin resistance.

REFERENCES

1. Bowman, J. S., Jr.; Burk, S. M., Jr.; Stough, H. P.; and Patton, J. M., Jr.: Correlation of Model and Airplane Spin Characteristics for a Low-Wing General Aviation Research Airplane. AIAA Paper No. 78-1477, 1978.

2. Stough, H. P., III; and Patton, J. M., Jr.: The Effect of Configuration Changes on Spin and Recovery Characteristics of a Low-Wing Spin Research Airplane. AIAA Paper No. 79-1786, 1979.

3. DiCarlo, D. J.; Stough, H. P., III; and Patton, J. M., Jr.: Effects of Discontinuous Drooped Wing Leading-Edge Modification on the Spinning Characteristics of a Low-Wing General Aviation Airplane. AIAA Paper No. 80-1843, 1980.

4. Bihrle, W., Jr.; and Bowman, J. S., Jr.: The Influence of Wing, Fuselage, and Tail Design on Rotational Flow Aerodynamics Data Obtained Beyond Maximum Lift with General Aviation Configurations. AIAA Paper No. 80-0455, 1980.

5. Staff of Langley Research Center: Exploratory Study of the Effects of Wing-Leading-Edge Modifications on the Stall/Spin Behavior of a Light General Aviation Airplane. NASA TP-1589, 1979.

6. Johnson, Joseph L., Jr.; Newsom, William A.; and Satran, Dale R.: Full-Scale Wind-Tunnel Investigation of the Effects of Wing Leading-Edge Modifications on the High Angle-of-Attack Aerodynamic Characteristics of a Low-Wing General Aviation Airplane. AIAA Paper No. 80-1844, 1980.

7. Kroeger, R. A.; and Feistel, T. W.: Reduction of Stall/Spin Entry Tendencies Through Wing Aerodynamic Design. SAE Paper No. 760481, Business Aircraft Meeting, 1976.

8. Bihrle, W., Jr.; and Mulcay, W.: Rotary Balance Data for a Typical Single-Engine General Aviation Design for an Angle-of-Attack Range of 8° to 35°. III - Effect of Wing Leading-Edge Modifications Model A. NASA CR-3102, 1979.

9. Burk, Sanger M., Jr.; and Wilson, Calvin F., Jr.: Radio-Controlled Model Design and Testing Techniques for Stall/Spin Evaluation of General-Aviation Aircraft. NASA TM-80510, 1975.

10. Glauert, H.: The Rotation of an Airfoil About a Fixed Axis. R and M 595, British A.C.A., 1919.

11. Knight, Montgomery: Wind-Tunnel Tests on Autorotation and the "Flat Spin". NACA Report 273, 1927.

TABLE 1. OUTBOARD DROOP CO-ORDINATES.

INBOARD SPAN STA. $y/b/2 = .55$ (BASED ON LOCAL CHORD)		TIP STATION (BASED ON LOCAL CHORD)	
X/C	Z/C	X/C	Z/C
.02441	.02816	.03424	.03093
.02181	.02726	.03080	.02872
.01953	.02666	.02737	.02666
.01709	.02549	.02392	.02449
.01465	.02432	.02049	.02168
.01221	.02295	.01706	.01888
.00977	.02148	.01362	.01649
.00732	.02021	.01018	.01362
.00488	.01855	.00675	.01115
.00244	.01689	.00332	.00793
0.00000	.01543	-.00011	.00346
-.00244	.01348	-.00353	.00065
-.00488	.01172	-.00695	-.00285
-.00732	.00977	-.01036	-.00746
-.00977	.00771	-.01378	-.01192
-.01221	.00498	-.01719	-.01681
-.01465	.00273	-.02059	-.02252
-.01709	0.00000	-.02397	-.03004
-.01953	-.00285	-.02732	-.04116
-.02197	-.00674	-.02859	-.05225
-.02441	-.01172	-.02711	-.06055
-.02686	-.01758	-.02358	-.06743
-.02832	-.02441	-.02007	-.07183
-.02686	-.03076	-.01657	-.07470
-.02441	-.03525	-.01309	-.07646
-.02197	-.03760	-.00961	-.07809
-.01953	-.03926	-.00614	-.07902
-.01709	-.04053	-.00267	-.07954
-.01465	-.04131	.00080	-.07978
-.01221	-.04199	.00426	-.08002
-.00977	-.04238	.00773	-.08026
-.00732	-.04287	.01119	-.08022
-.00488	-.04297	.01465	-.07977
-.00244	-.04307	.01811	-.07946
0.00000	-.04316	.02157	-.07928
.00977	-.04326	.02503	-.07883
.01953	-.04346	.02848	-.07849
.02930	-.04375	.03194	-.07820
.04883	-.04414	.03540	-.07789
.06836	-.04473	.04232	-.07740
.08789	-.04521	.05616	-.07559
.10742	-.04580	.06999	-.07433
.12695	-.04619	.09767	-.07168
.14648	-.04678	.12534	-.06862

TABLE 1. CONCLUDED.

INBOARD SPAN STA. $y/_{b/2} = .55$ (BASED ON LOCAL CHORD)		TIP STATION (BASED ON LOCAL CHORD)	
X/C	Z/C	X/C	Z/C
.16602	-.04736	.15301	-.06569
.18555	-.04775	.18068	-.06262
.20508	-.04824	.20835	-.05983
.22461	-.04883	.23602	-.05705
.23680	-.04919	.26369	-.05398
		.29136	-.05092

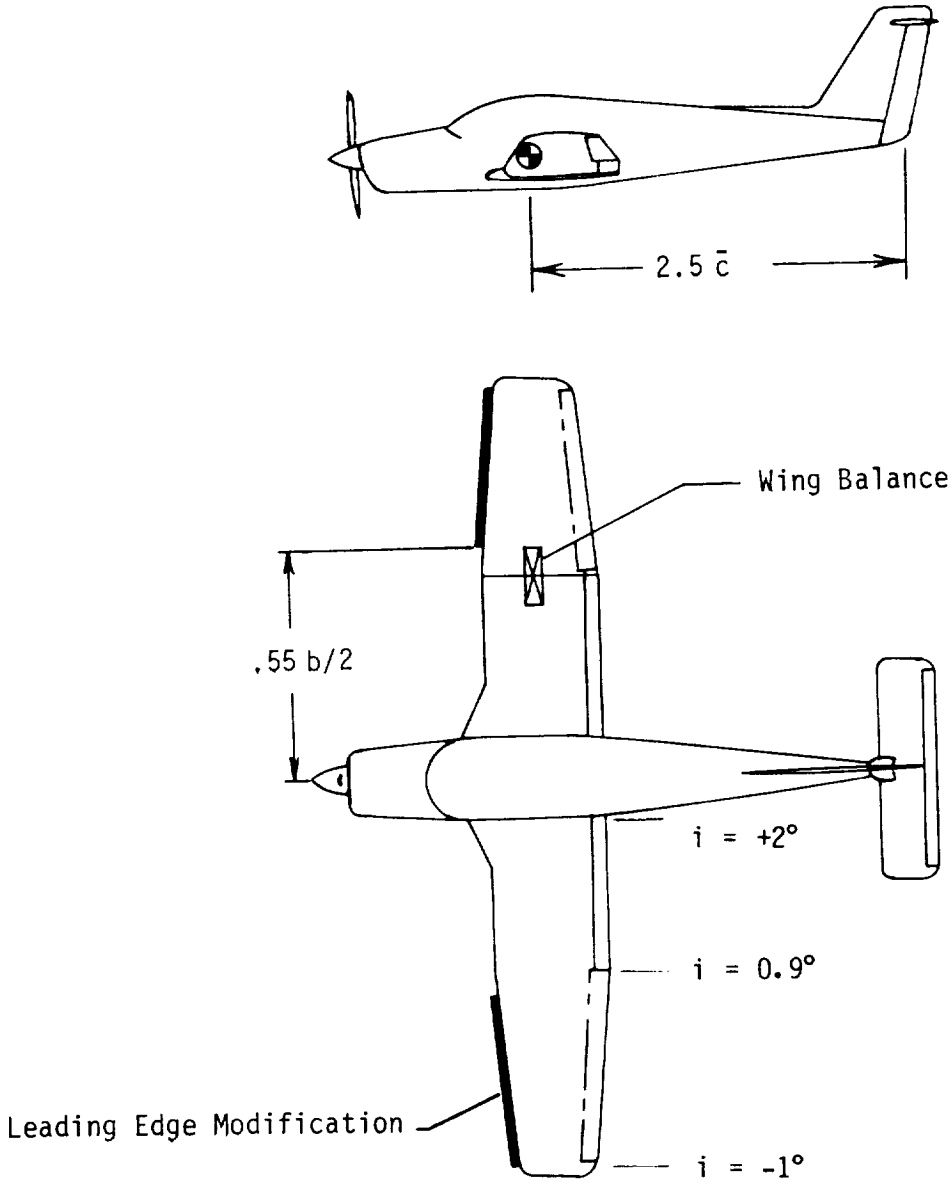

$S = 4.825\ ft^2$

$b = 5.904$ ft

$\bar{c} = .8639$ ft

wing airfoil 65_2-415 (modified)

Figure 1. - Model geometric characteristics.

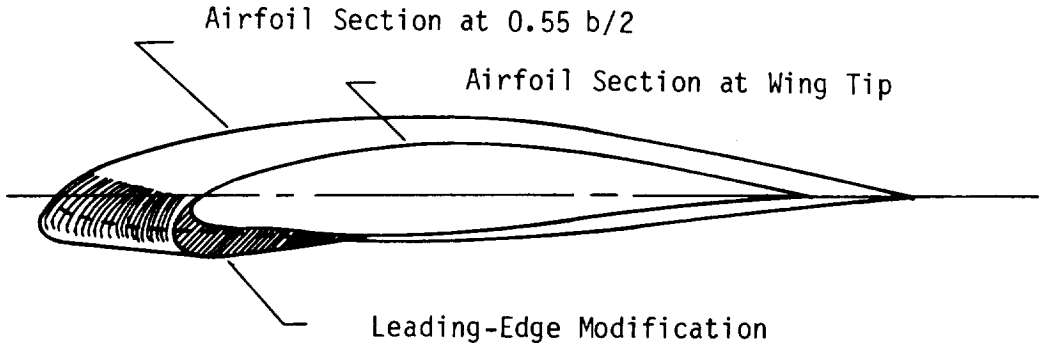

Co-ordinates shown in Table 1

Figure 2. - Droop geometry and installation on wing

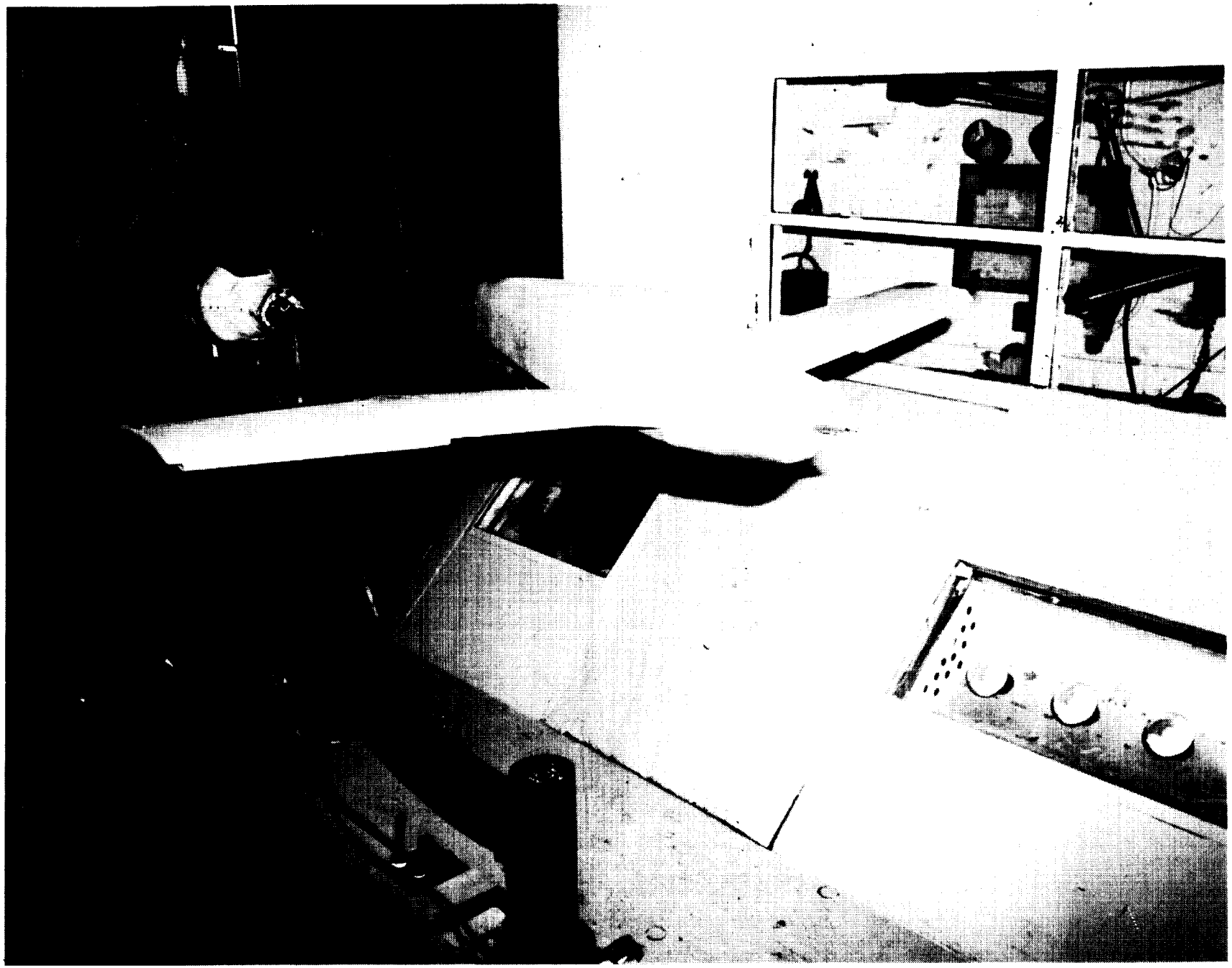

Figure 3.- Model installation in the Langley 12-Foot Low-Speed Wind Tunnel

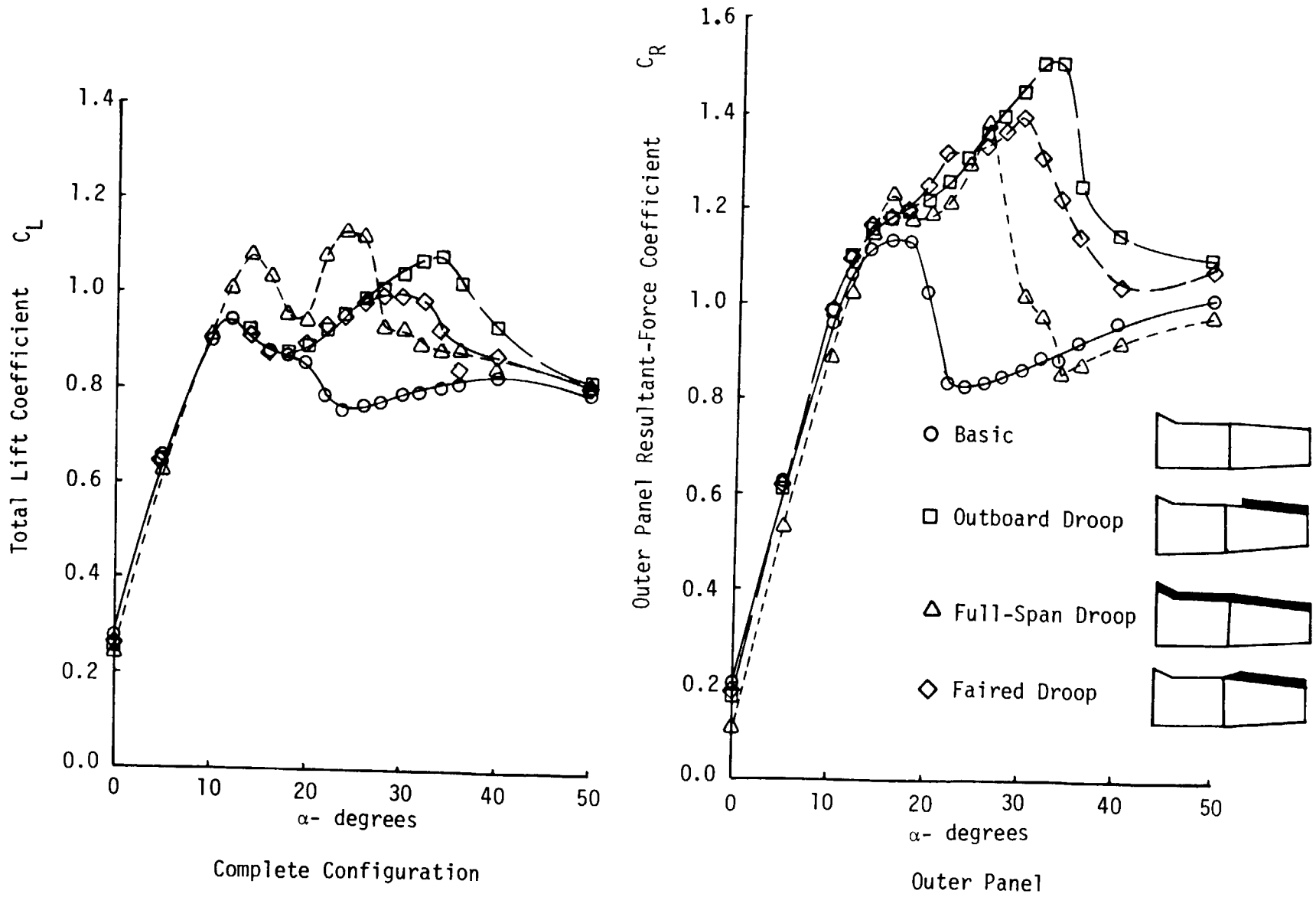

Figure 4.- Variation of total lift and outer panel resultant-force coefficient for different droop configurations.

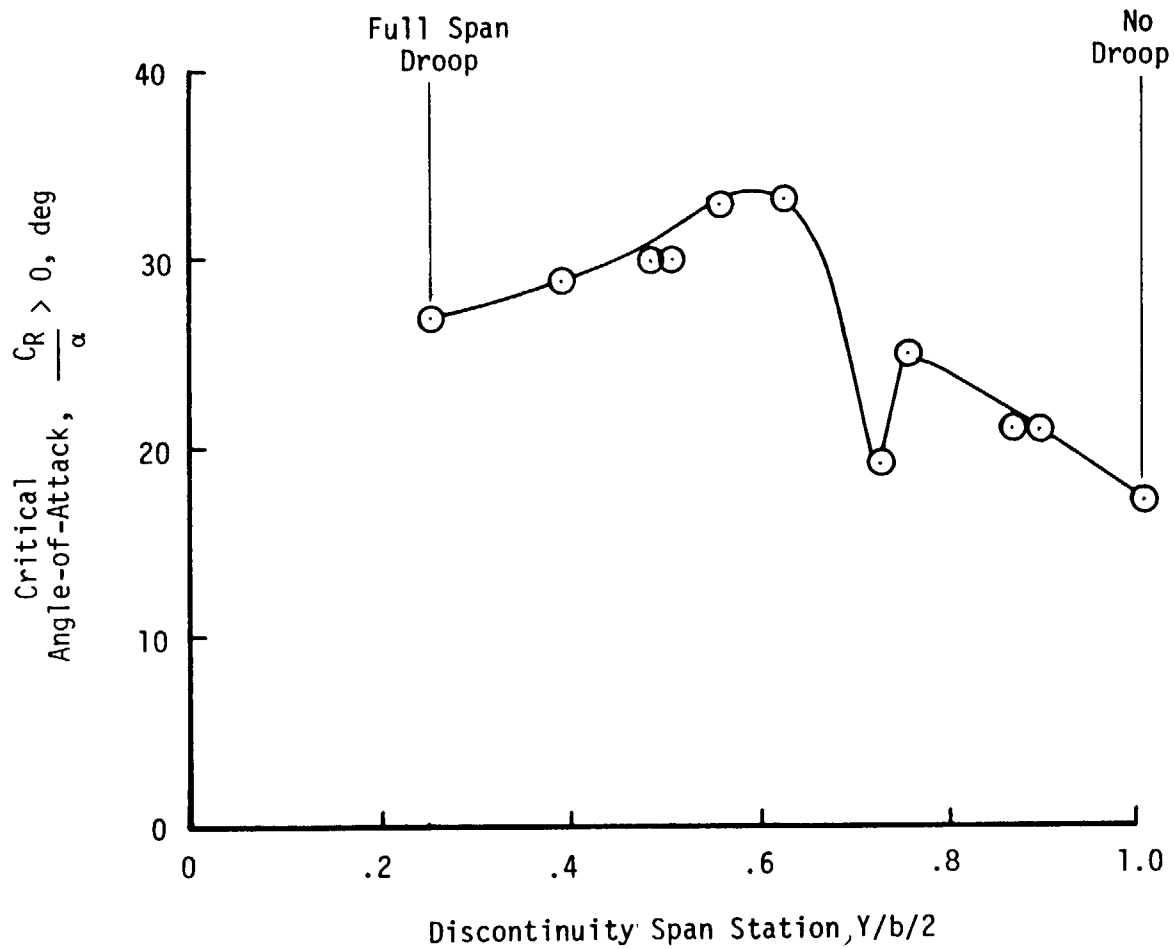

Figure 5. - Effect of outboard droop discontinuity location on critical angle of attack.

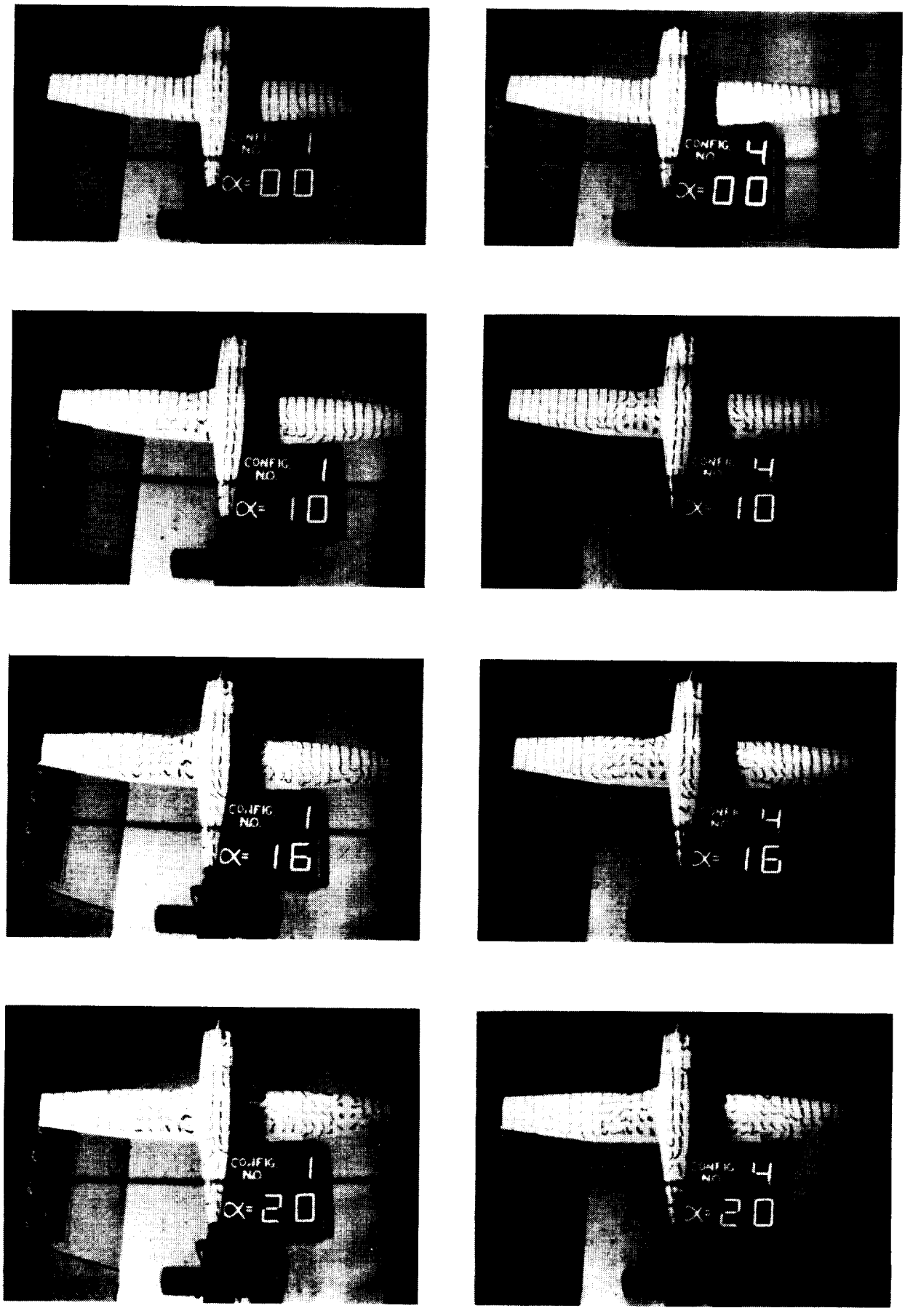

a) Basic

b) Outboard Droop

Figure 6.- Tuft photographs of basic and outboard droop configurations

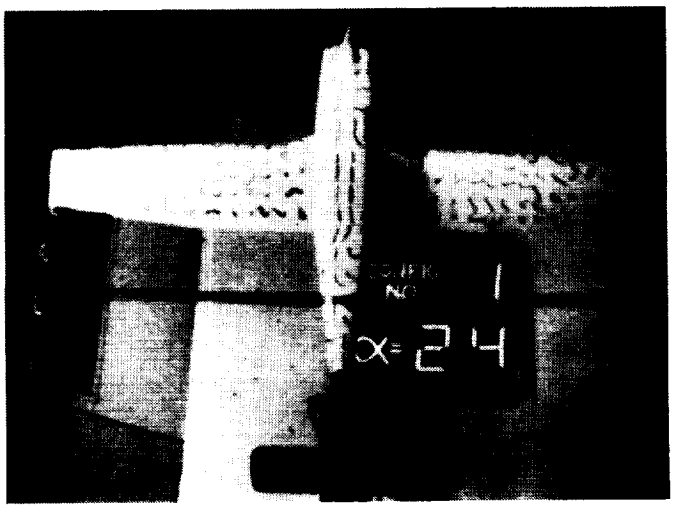

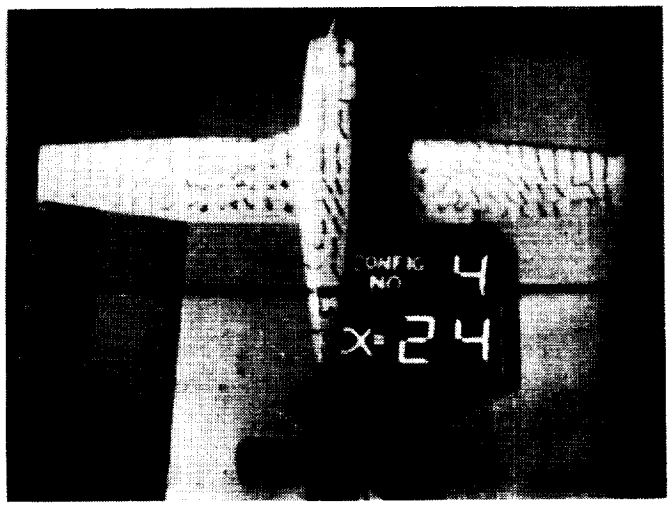

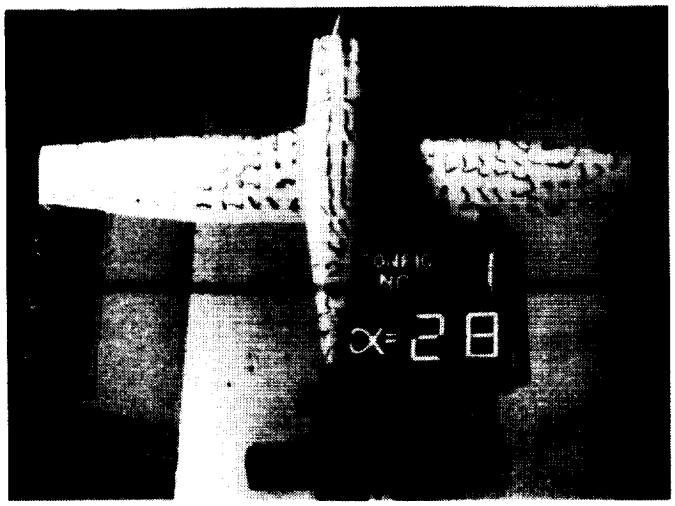

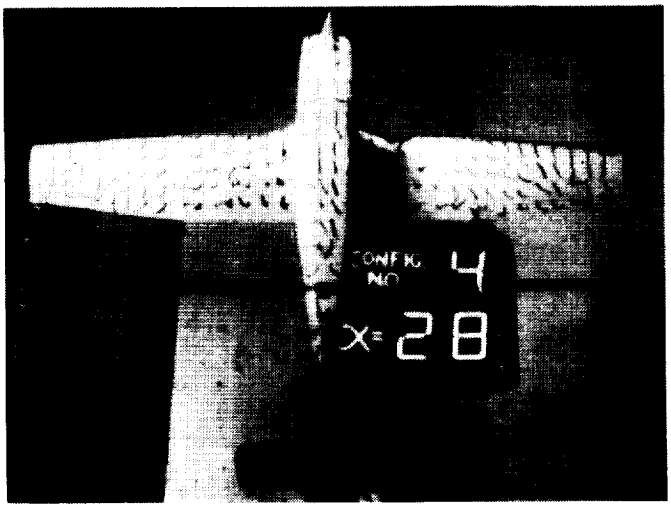

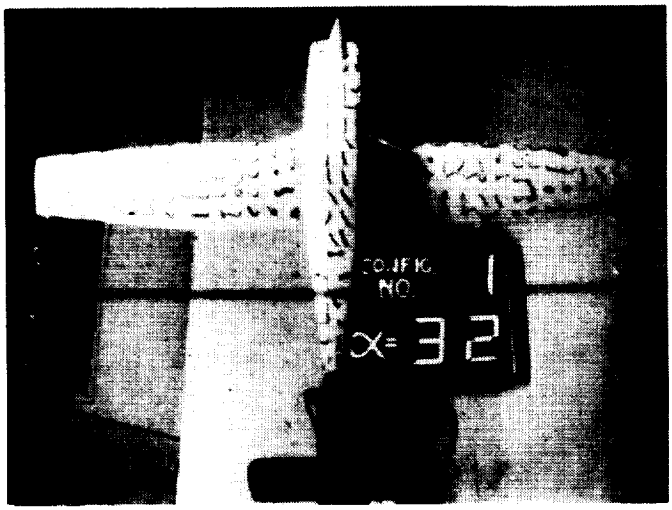

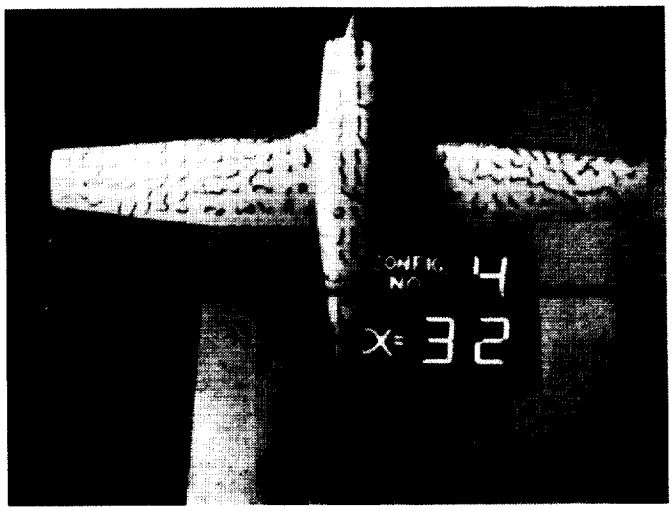

a) Basic

b) Outboard Droop

Figure 6. Concluded.

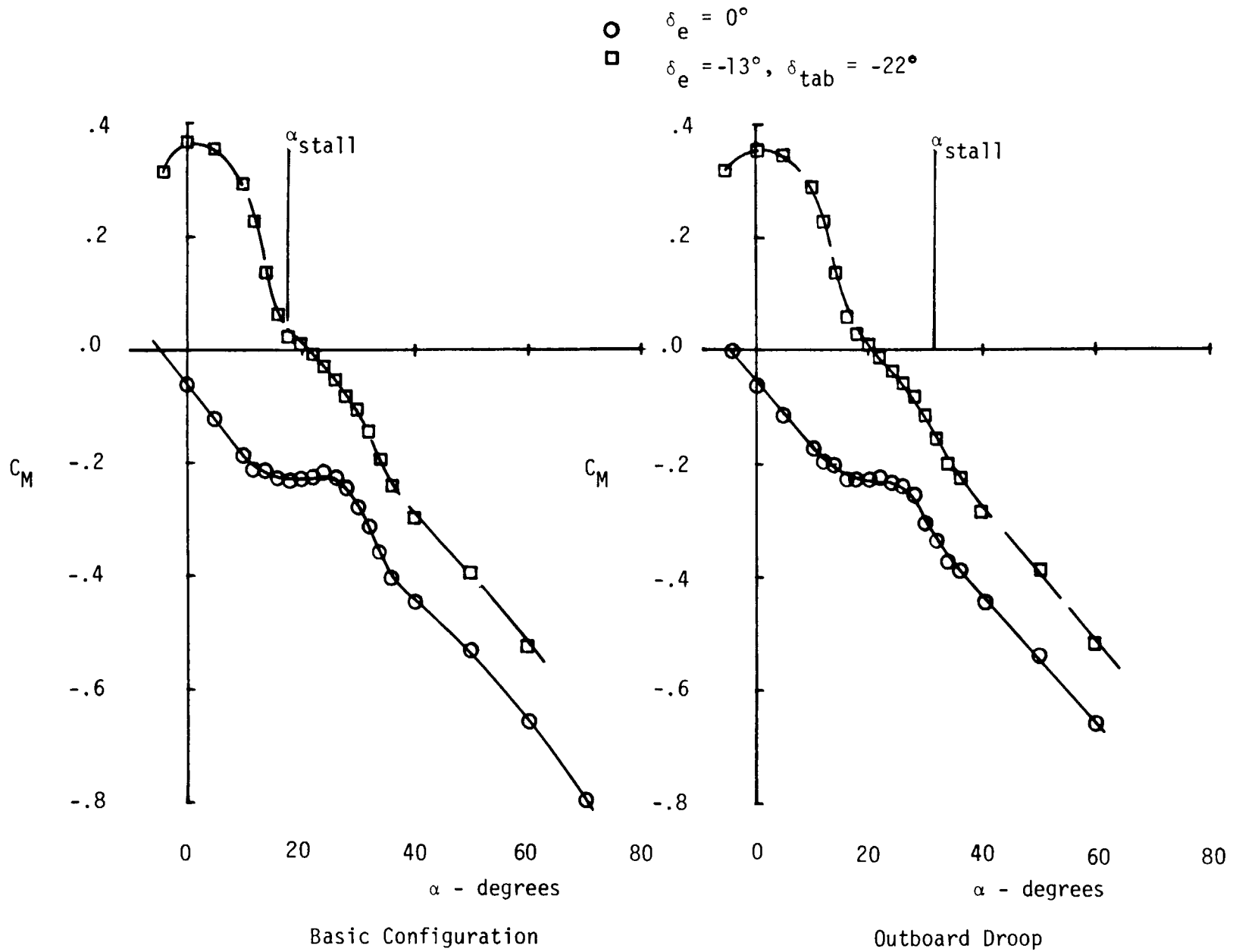

Figure 7.- Effect of maximum elevator deflection on pitching-moment characteristics.

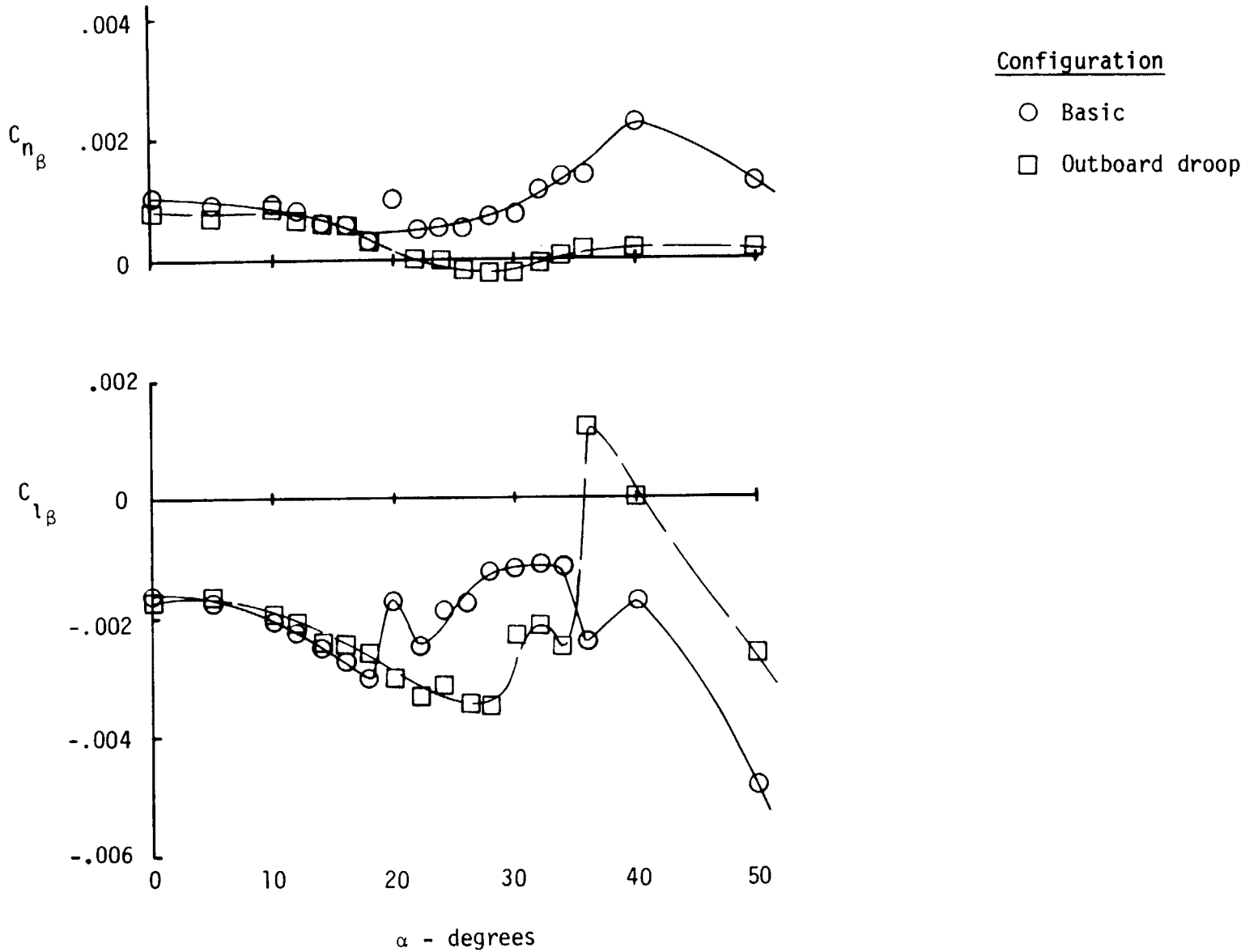

Figure 8.- Effect of outboard leading-edge droop on lateral-directional stability characteristics.

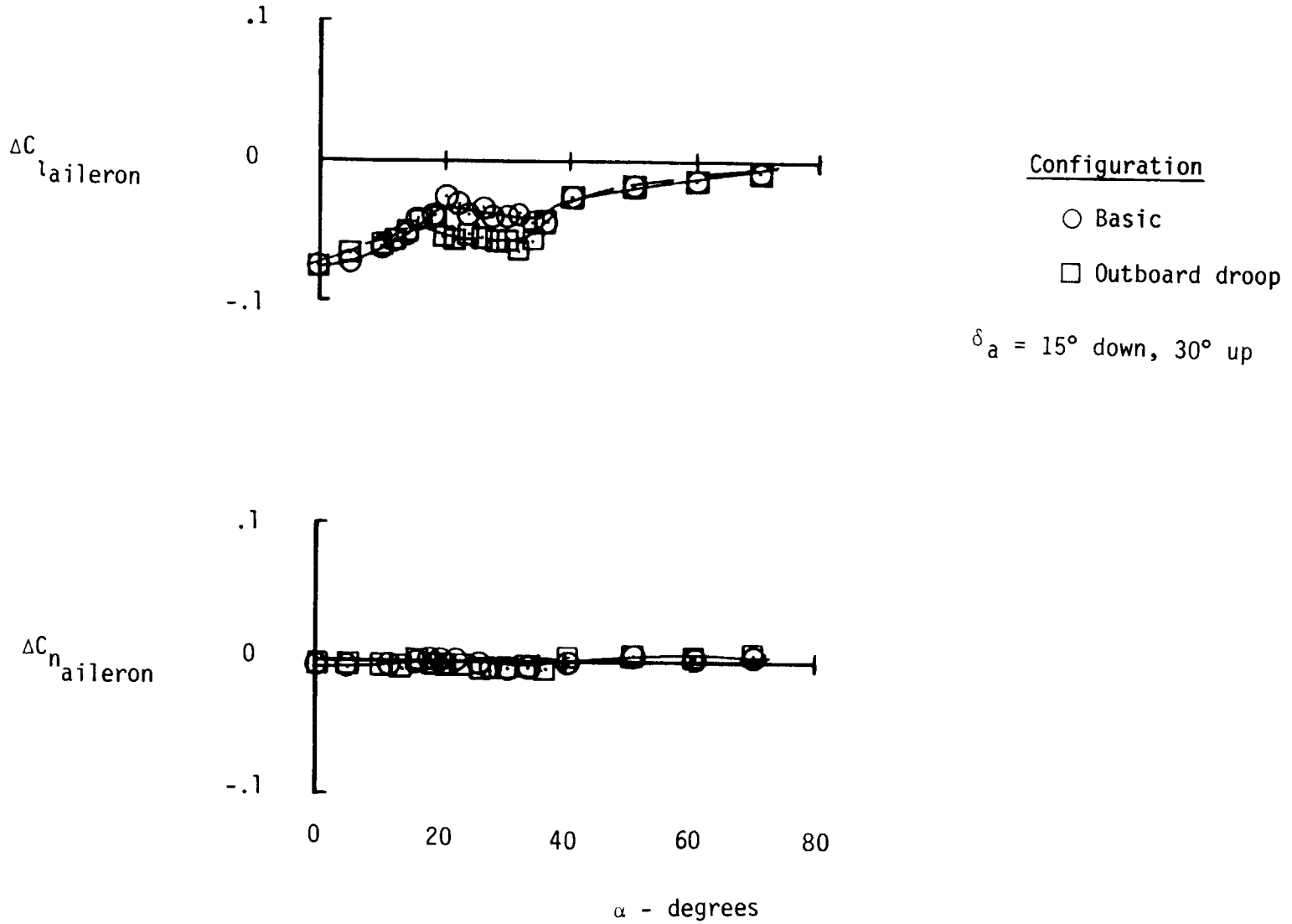

Figure 9.- Effect of full aileron deflection on rolling- and yawing-moment characteristics.

1. Report No.	2. Government Accession No.	3. Recipient's Catalog No.
NASA CR-3636		

4. Title and Subtitle	5. Report Date
WIND-TUNNEL INVESTIGATION OF EFFECTS OF WING-LEADING-EDGE MODIFICATIONS ON THE HIGH ANGLE-OF-ATTACK CHARACTERISTICS OF A T-TAIL LOW-WING GENERAL-AVIATION AIRCRAFT	November 1982
	6. Performing Organization Code

7. Author(s)	8. Performing Organization Report No.
E. Richard White	
	10. Work Unit No.

9. Performing Organization Name and Address	11. Contract or Grant No.
Kentron International, Inc. Kentron Technical Center 3221 N. Armistead Avenue Hampton, VA 23666	NAS1-16000
	13. Type of Report and Period Covered Contractor Report
12. Sponsoring Agency Name and Address National Aeronautics and Space Administration Washington, DC 20546	14. Sponsoring Agency Code

15. Supplementary Notes

Langley Technical Monitor: Joseph L. Johnson, Jr.

16. Abstract Exploratory tests have been conducted in the NASA-Langley Research Center's 12-Foot Low-Speed Wind Tunnel to evaluate the application of wing-leading-edge devices on the stall-departure and spin resistance characteristics of a 1/6-scale model of a T-tail general-aviation aircraft. The model was force tested with an internal strain-gauge balance to obtain aerodynamic data on the complete configuration and with a separate wing balance to obtain aerodynamic data on the outer portion of the wing.

The addition of the outboard leading-edge droop eliminated the abrupt stall of the wingtip and maintained or increased the resultant-force coefficient up to about α = 32 degrees. This change in slope of the resultant-force coefficient curve with angle of attack from negative to positive values at higher angles of attack has been shown to be important for eliminating autorotation and for providing spin resistance.

17. Key Words (Suggested by Author(s))	18. Distribution Statement
Spin resistance Stall resistance Wing-leading-edge modifications General Aviation	Unclassified - Unlimited Subject Category 02

19. Security Classif. (of this report)	20. Security Classif. (of this page)	21. No. of Pages	22. Price
Unclassified	Unclassified	24	A02

For sale by the National Technical Information Service, Springfield, Virginia 22161

NASA-Langley, 1982